

# ATLAS high- $p_T$ measurements in lead-lead collisions

Zvi Citron on behalf of the ATLAS Collaboration

Weizmann Institute of Science, Rehovot Israel

E-mail: [zvi.citron@weizmann.ac.il](mailto:zvi.citron@weizmann.ac.il)

**Abstract.** Measurements of high- $p_T$  processes in lead-lead collisions can provide insight into the physics responsible for the quenching of jets in the quark gluon plasma. Results are presented from ATLAS measurements of single jet suppression, both inclusively and as a function of the azimuthal angle of the jets with respect to the elliptic flow plane, single jet fragmentation, and gamma-jet correlations. Implications of the results are discussed. Results are also presented for measurements of photon and  $Z$  boson production that provide essential tests on calculations of hard scattering rates using binary collision scaling.

Lead-lead collisions at  $\sqrt{s_{NN}} = 2.76$  TeV at the Large Hadron Collider (LHC) provide the opportunity to study strongly interacting matter at the highest temperatures achieved in a laboratory setting. The ATLAS experiment has a robust heavy-ion program to take advantage of this opportunity. In the 2010 and 2011 LHC runs, yielding approximately  $10 \mu\text{b}^{-1}$  and  $0.15 \text{nb}^{-1}$ , respectively, the ATLAS experiment has made a set of measurements that form an emerging picture of the hot dense matter created in heavy ion collisions. These measurements include hard probes such as photons [1, 2],  $Z$  bosons [3, 4], and single and di-jet measurements [5, 6, 7, 8]. Some of the present discussion appears in [9].

The ATLAS detector [10] at the LHC covers nearly the entire solid angle around the collision point. It consists of an inner tracking detector surrounded by a thin superconducting solenoid, electromagnetic and hadronic calorimeters, and a muon spectrometer incorporating three superconducting toroid magnet systems. The inner-detector system (ID) is immersed in a 2 T axial magnetic field and provides charged particle tracking in the pseudorapidity range  $|\eta| < 2.5$ . The high-granularity silicon pixel detector covers the vertex region and is surrounded by the silicon microstrip tracker and transition radiation tracker. The calorimeter system covers the range  $|\eta| < 4.9$ . Within the region  $|\eta| < 3.2$ , electromagnetic calorimetry is provided by barrel and endcap high-granularity lead liquid-argon (LAr) calorimeters, with an additional thin LAr presampler covering  $|\eta| < 1.8$ . Forward calorimeters (FCal) are located in the range  $3.1 < |\eta| < 4.9$ . The muon spectrometer comprises separate trigger and high-precision tracking chambers that measure the deflection of muons in a magnetic field generated by superconducting air-core toroids. The precision tracking chamber system covers the region  $|\eta| < 2.7$  with trigger coverage in the range  $|\eta| < 2.4$ .

High momentum particles allow us to probe the properties of the dense medium created in heavy ion collisions, and how color sensitive objects interact with it. Measurements of inclusive single particle spectra as well as two particle correlations have suggested that jets are being “quenched” in the medium, and much effort has been made to understand the mechanisms of this quenching. The suppression of jet production may be quantified using the nuclear modification

factor,  $R_{CP}$ :

$$R_{CP} = \frac{\langle N_{coll} \rangle (P) (1/N_{evt,C}) d^2 N_C / d\eta dp_T}{\langle N_{coll} \rangle (C) (1/N_{evt,P}) d^2 N_P / d\eta dp_T} \quad (1)$$

where  $C$  and  $P$  refer to central and peripheral event classes, respectively, and  $\langle N_{coll} \rangle$  is the mean number of binary nucleon-nucleon collisions in a given centrality class. Figure 1 shows the  $R_{CP}$  of jets as a function of the mean number of nucleons participating in a Pb+Pb collision,  $\langle N_{part} \rangle$ , clearly demonstrating the suppression of the overall jet yield. The suppression observed is independent of the jet  $p_T$  within the experimental uncertainties.

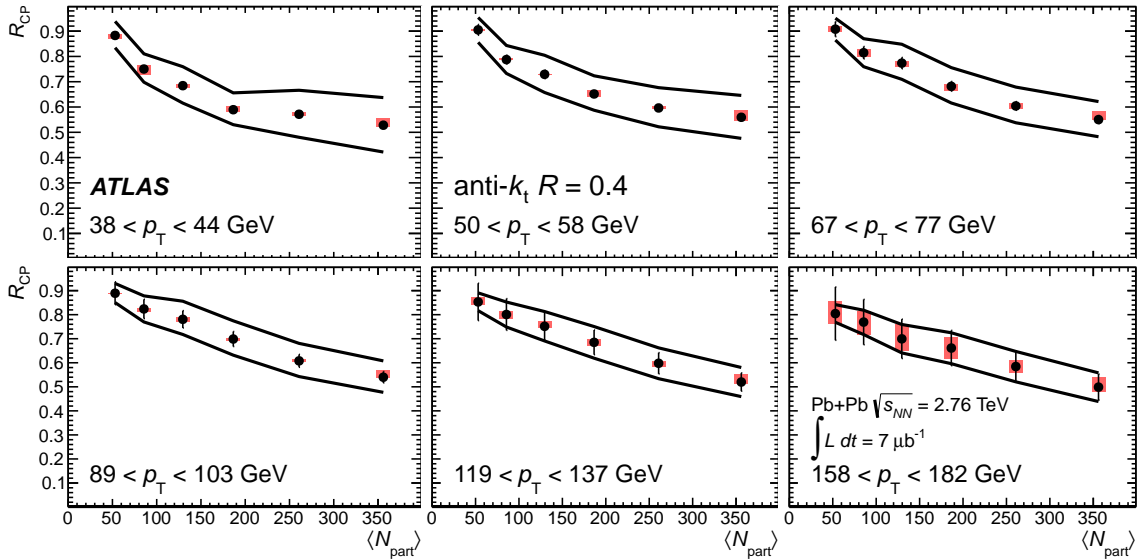


**Figure 1.**  $R_{CP}$  as a function of  $\langle N_{part} \rangle$  for  $R = 0.4$  anti- $k_t$  jets in six  $p_T$  bins. The jet spectra are unfolded to correct for any distortions due to detector resolution and underlying event fluctuations. The error bars indicate statistical errors from the unfolding; the shaded boxes indicate point-to-point systematic errors that are only partially correlated. The solid lines indicate systematic errors that are fully correlated between all points. The horizontal errors indicate systematic uncertainties on  $\langle N_{part} \rangle$ . Figure is from reference [5].

Further understanding of how jets interact with the medium is provided by considering the azimuthal distribution of jets. The di-jet energy asymmetry [8] and jet  $R_{CP}$  show that there is significant quenching, however this is averaged over all in-medium path lengths the jets may be probing. In order to directly examine the path length dependence of jet modification the distribution of jets relative to the reaction plane of the collision was measured, which reflects the anisotropy of the reaction region in which the medium formed. Similarly defined to the  $v_2$  used to measure the flow,  $v_2^{jet}$  measures anisotropy of jet yields relative to the amount of medium they traverse. Figure 2 shows a significant non-zero  $v_2^{jet}$  as a function of  $p_T$ .

To study the mechanisms of the quenching we may measure the structure of the reconstructed jets themselves. A possible mechanism of jet suppression involves radiated gluons from the leading parton being shunted out of the jet cone due to multiple scattering with the medium, which would lead to a dependence on the jet cone size of the jet  $R_{CP}$ . This trend is seen in the  $R_{CP}$  measured for jets reconstructed with different radii [5].

To further understand the structure of the jets and possible mechanisms of quenching, we

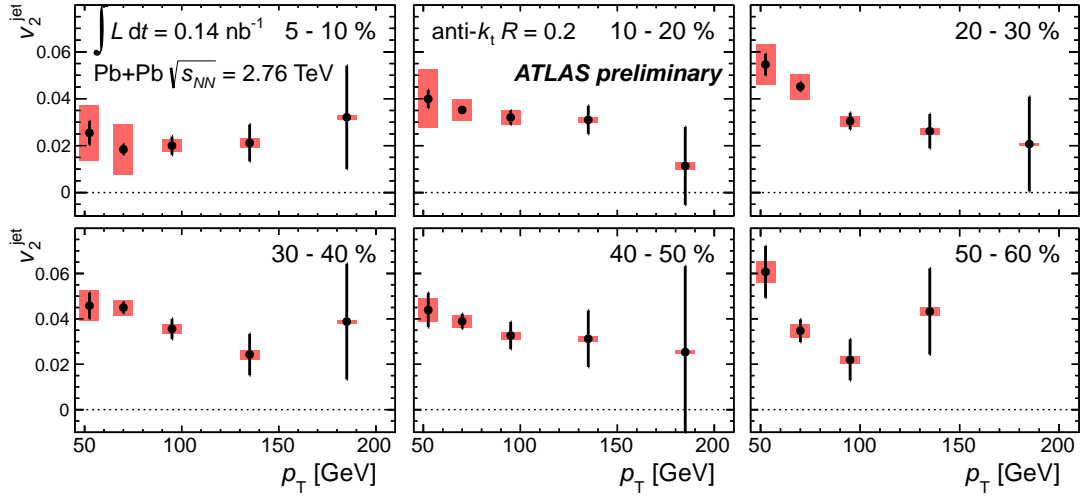


**Figure 2.**  $v_2^{jet}$  as a function of  $p_T$  for several centrality bins. The error bars on the points indicate statistical uncertainties while the shaded bands represent systematic uncertainties. Figure is from reference [7].

may consider the fragmentation function of the jets and its central to peripheral ratio:

$$D(z) = \frac{p_T^{particle}}{p_T^{jet}} \cos(\sqrt{\Delta\eta^2 + \Delta\phi^2}), R_{D(z)} = \frac{D(z)|_{central}}{D(z)|_{peripheral}} \quad (2)$$

where particle refers to reconstructed tracks inside the reconstructed jet cone with  $\Delta\eta$  and  $\Delta\phi$  the distance between the particle and jet directions. The ratio  $R_{D(z)}$  reflects the increasing modification of the jet substructure with centrality. Figure 3 shows  $R_{D(z)}$  for three centrality intervals, and indicates that within the experimental uncertainties the leading particle at high  $z$  is unmodified but rather that only lower momentum particles at mid  $z$  are.

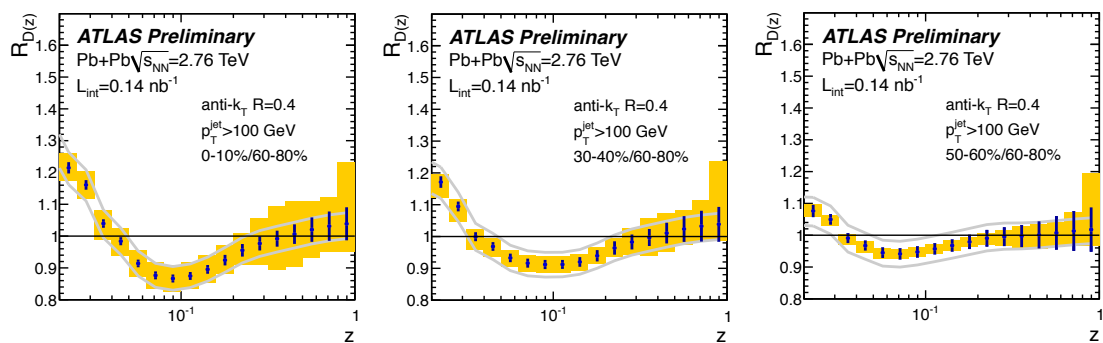


**Figure 3.** Ratios of  $D(z)$  for three bins in collision centrality to those in peripheral (60-80%) collisions,  $R_{D(z)}$ , for  $R = 0.4$  jets. The error bars on the data points indicate statistical uncertainties while the shaded bands indicate systematic uncertainties that are uncorrelated or partially correlated between points. The solid lines indicate systematic uncertainties that are 100% correlated between points. Figure is from reference [6].

In contrast to the modification of color sensitive objects discussed above, color neutral electroweak bosons are expected to be unmodified in the medium. To confirm this as well

as the  $\langle N_{\text{coll}} \rangle$  scaling assumptions, we measure photons and  $Z$  bosons. The boson yields are compared to pQCD models of production that include no modification due to the presence of the medium or to the nuclear parton distribution functions, and show good agreement [2, 3].

The color neutral bosons provide an unbiased baseline from which to measure jet modification in the medium. In a boson+jet event the boson allows direct access to the initial hard scattering which produced both the boson and the jet, and is thus a useful baseline from which to evaluate the jet modification. We may consider the azimuthal distribution of boson+jet pairs and the momentum fraction  $p_{\text{T}}^{\text{jet}}/p_{\text{T}}^{\text{boson}}$ . As in the di-jet case the azimuthal distribution is consistent between central Pb+Pb events and an unmodified pQCD model, however selecting azimuthally correlated events there is a reduction in the mean  $p_{\text{T}}$  of the jet compared to the boson  $p_{\text{T}}$ . These events have been studied for the  $Z$  boson and photon+jet cases [4, 2]. The means of the  $p_{\text{T}}^{\text{jet}}/p_{\text{T}}^{\text{boson}}$  and the boson+jet yield normalized by the number of bosons are shown in Figure 4 for photons from both the data and simulation. Although the uncertainties are large (especially in the  $Z$  boson case) these measurements show a qualitative result consistent with jet quenching and hold promise for future precision studies.

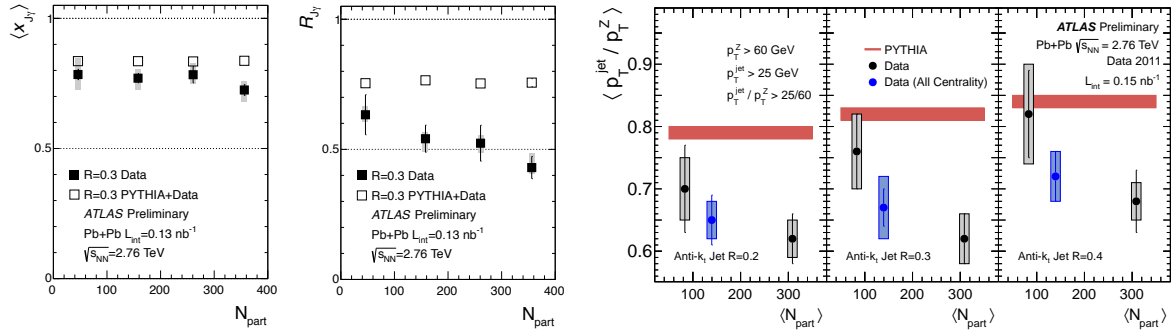


**Figure 4.** Far left: The mean energy fraction  $\langle x_{J_\gamma} \rangle = \langle p_{\text{T}}^{\text{jet}}/p_{\text{T}}^{\text{photon}} \rangle$  from fully corrected and unfolded distributions calculated as a function of jet radius ( $R = 0.2$  and  $R = 0.3$ ), and for each radius as a function of  $\langle N_{\text{part}} \rangle$ . Center: The integrated yield of jets per photon  $R_{J_\gamma}$ . The figures are from reference [2]. Far right: The extracted means from the  $p_{\text{T}}^{\text{jet}}/p_{\text{T}}^Z$  distributions of the fully corrected data plotted as a function of  $\langle N_{\text{part}} \rangle$ . The systematic uncertainties are largely correlated across the  $\langle N_{\text{part}} \rangle$  bins. The width of the PYTHIA band represents its uncertainty. The points at  $\langle N_{\text{part}} \rangle = 140$  refer to 0-80% centrality. The figures are from reference [4]. In all figures bars represent statistical uncertainties, and shaded boxes systematic uncertainties. The data are compared to PYTHIA events embedded into minimally biased data events.

## References

- [1] ATLAS Collaboration 2012 ATLAS-CONF-2012-051, <https://cdsweb.cern.ch/record/1451913>
- [2] ATLAS Collaboration 2012 ATLAS-CONF-2012-121, <https://cdsweb.cern.ch/record/1473135>
- [3] ATLAS Collaboration 2013 *Phys. Rev. Lett.* **110** 02231
- [4] ATLAS Collaboration 2012 ATLAS-CONF-2012-119, <https://cds.cern.ch/record/1472941>
- [5] ATLAS Collaboration 2013 *Phys. Lett. B* **719** 220-241
- [6] ATLAS Collaboration 2012 ATLAS-CONF-2012-115, <http://cds.cern.ch/record/1472936>
- [7] ATLAS Collaboration 2012 ATLAS-CONF-2012-116, <http://cds.cern.ch/record/1472938>
- [8] ATLAS Collaboration 2010 *Phys. Rev. Lett.* **105** 252303
- [9] Citron Z (on behalf of the ATLAS Collaboration) 2013 *J. Phys.: Conf. Series* **455** 012011
- [10] ATLAS Collaboration 2008 JINST **3** S08003
- [11] Cacciari M, Salam G P, and Soyez G 2008 JHEP **0804** 063